

## PLASMON INTERACTIONS IN METALLIC GRATINGS: $\omega$ - AND $k$ -MINIGAPS AND THEIR CONNECTION WITH POLES AND ZEROS

E. POPOV

*Institute of Solid State Physics, Bulgarian Academy of Sciences, Blvd. Lenin 72, Sofia 1784, Bulgaria*

Received 17 April 1989; accepted for publication 6 July 1989

A numerical analysis is presented of two types of minigaps:  $\omega$ - and  $k$ -gap that are formed in the reflectivity dips when two oppositely propagating plasmon surface waves (PSW's) are excited simultaneously. Their connection with complex trajectories of poles and zeros is revealed: an  $\omega$ -gap is formed when splitting of poles is observed and a  $k$ -gap only exists when a splitting of zeros occurs.

### 1. Introduction

It is well-known that when a PSW propagates along a metallic grating, the corrugation modifies its propagation constant. This influence is especially pronounced in the so-called "mini-gap" region, where the grating couples two oppositely propagating surface waves [1]. This causes an energy transfer and a sharp increase of the imaginary part of the PSW propagating constant  $\alpha^p$  is observed even in the case of lossless media. Thus a forbidden gap in the dispersion curve appears ( $\omega$ -gap).

Very recently it has been discovered [2] that at some conditions a  $k$ -gap, rather than  $\omega$ -gap, can be formed. Tran et al. [3] have shown that the formation of  $\omega$ - or  $k$ -gaps is independent on the excitation conditions but is determined mainly by the correlation between the strength of the direct coupling of the two PSW's, their coupling to the radiation diffraction order( $s$ ) and the other types of losses.

The aim of this paper is to give a physical interpretation of both types of mini-gaps. For this sake their connection with the complex trajectories of poles (solutions of dispersion relation) and zeros of the reflectivity is revealed.

### 2. Phenomenological approach

This section contains a brief review of the phenomenological approach to the anomalies of diffraction gratings [4]. This is necessary in order to understand the physical background of the results presented in the next section.

The existence of a surface wave on a flat boundary can be expressed mathematically with a pole  $\alpha^P(\lambda)$  of the scattering matrix, i.e. a solution of the homogeneous problem. As it can easily be shown, the corrugation of the surface with an amplitude  $h$  leads not only to a modification but to a multiplication of the pole  $\alpha^P(\lambda, h)$ . In particular, if the wavelength to period ratio  $\lambda/d$  is properly chosen, then some of these newly formed poles (namely  $\alpha_0^P$ ) can appear in the light cone defined by  $|\alpha| < 1$ , where  $\alpha \equiv k_{\parallel}/k$ ,  $k_{\parallel}$  is the wavevector component in the grating plane,  $k = 2\pi/\lambda$  being the wavenumber. Then the surface wave can be excited with a plane wave incident at an angle  $\theta = \arcsin\alpha$  through the  $m$ th diffraction order, provided the phase conditions are satisfied:

$$\alpha = \text{Re}(\alpha_0^P) \equiv \text{Re}(\alpha^P + m\lambda/d).$$

In that case all the elements of the scattering matrix have pole  $\alpha_0^P$ , i.e. they are proportional to  $(\alpha - \alpha_0^P)^{-1}$ . For this reason anomalies can be observed in the diffraction efficiencies.

On the other hand on flat surface (groovedepth  $h=0$ ) there are no anomalies. Thus for  $h=0$  the pole in the denominator  $(\alpha - \alpha_0^P)$  of the matrix elements must be exactly compensated by a zero  $\alpha_0^Z = \alpha_0^P$  of their numerator. As  $h \neq 0$ , the pole and the zero are split and the amplitude  $a_0^d$  of, for example, the zeroth reflected order can be expressed in the following general form

$$a_0^d = c_0(\lambda, h) \frac{\alpha - \alpha_0^Z(\lambda, h)}{\alpha - \alpha_0^P(\lambda, h)}, \quad (1)$$

where  $c_0$ ,  $\alpha_0^Z$  and  $\alpha_0^P$  are slowly varying functions of  $h$  and  $\lambda$ . Some important remarks on eq. (1) are worth noting:

(1) It must be pointed out that the existence of the zero  $\alpha_0^Z$  in the numerator of eq. (1) is quite important. It describes the fact that resonance anomalies (e.g. PSW excitation) are characterized usually by a dip, rather than by a sharp peak of diffraction efficiency (as it should be if only a pole exists).

(2) Let us denote the real part of the pole by  $\alpha_0^{P'}$  and its imaginary part by  $\alpha_0^{P''}$ . For highly conducting metals usually [4]:

$$\text{Re}(\alpha_0^Z) \approx \alpha_0^{P'}, \quad (2)$$

thus the position of the minimum of reflectivity is a very good criterion for determination of  $\alpha_0^{P'}$ .

If condition (2) is fulfilled, together with:

$$|\text{Im}(\alpha_0^Z)| \ll \alpha_0^{P''}, \quad (3)$$

then eq. (1) can be written in a simplified form:

$$|a_0^d|^2 = |c_0|^2 \frac{(\alpha - \alpha_0^{P'})^2}{(\alpha - \alpha_0^{P'})^2 + (\alpha_0^{P''})^2}. \quad (1')$$

In that case the halfwidth  $\Delta$  of the dip,

$$\Delta = 2\alpha_0^{\prime\prime}, \quad (4)$$

is just proportional to the decay constant  $2k\alpha_0^{\prime\prime}$ .

(3) If conditions (2) and (3) are not fulfilled, then a straight connection cannot be drawn between the position and halfwidth of diffraction efficiency minimum at one hand, and the propagation and decay constants of the excited wave at the other hand.

A typical example can be found further in section 3.1 (figs. 1c and 2): there are no peculiarities in the spectral behaviour of the pole, while the gap in the trajectories of the zeros leads to the appearance of a  $k$ -gap in the  $\omega$ - $k$  dependence of the reflectivity. What one could measure would be the position of the zero, rather than the value of plasmon propagation constant.

In such case it is possible to find the exact values of  $\alpha_0^{\prime}$  and  $\alpha_0^{\prime\prime}$  by numerical fitting of the reflectivity curve with eq. (1), where  $c_0$ ,  $\alpha_0^z$  and  $\alpha_0^p$  are unknown parameters.

When there is interaction of anomalies, second pole and zero have to be included in eq. (1) and the connection of the reflectivity curve with the position of both poles and both zeros is more complicated.

### 3. Numerical results

In our further calculations we have used a computer code based on the rigorous differential formalism of Chandezon et al. [5], generalized to work for complex values of  $\alpha$ . This method proves to be very efficient [6] for practically all kinds of grating.

Two types of aluminum gratings are investigated: (a) with a symmetrical sinusoidal profile containing only  $\pm 1$ st Fourier component, and (b) with a non-sinusoidal (asymmetrical and symmetrical) profile containing  $\pm 1$ st and  $\pm 2$ nd Fourier components.

The period  $d = 0.63 \mu\text{m}$  is one and the same for the two gratings and is chosen to provide for the existence of the two poles and two zeros of the scattering matrix, i.e. a simultaneous excitation of the two PSW's propagating in opposite directions for red wavelengths. The aluminum refractive index  $n = 1.378 + i7.616$  is taken to be independent of  $\lambda$  in the investigated spectral region (615–660 nm). Its slight dispersion should change the presented results insignificantly.

#### 3.1. Sinusoidal profile

Figs. 1a–1d present the results of numerical spectral tracing of two poles and two zeros for sinusoidal grating with profile function  $f(x)$  defined by:

$$f(x) = (h_1/2) \sin(2\pi x/d), \quad (5)$$

at different values of grating amplitude  $h_1$ :

Away from the coupling region ( $\lambda \approx 635$  nm) the imaginary parts of the pole and the zero are practically independent on the wavelength and are determined by the groovedepth value:  $\text{Im}(\alpha_0^p)$  is growing slowly with  $h_1$  due to the increase of absorption (and diffraction, if any) losses [7];  $\text{Im}(\alpha_0^z)$  decreases with the same rate, i.e.  $\text{Im}(\alpha_0^p) + \text{Im}(\alpha_0^z) \approx \text{const}(h_1)$ . At a given groovedepth

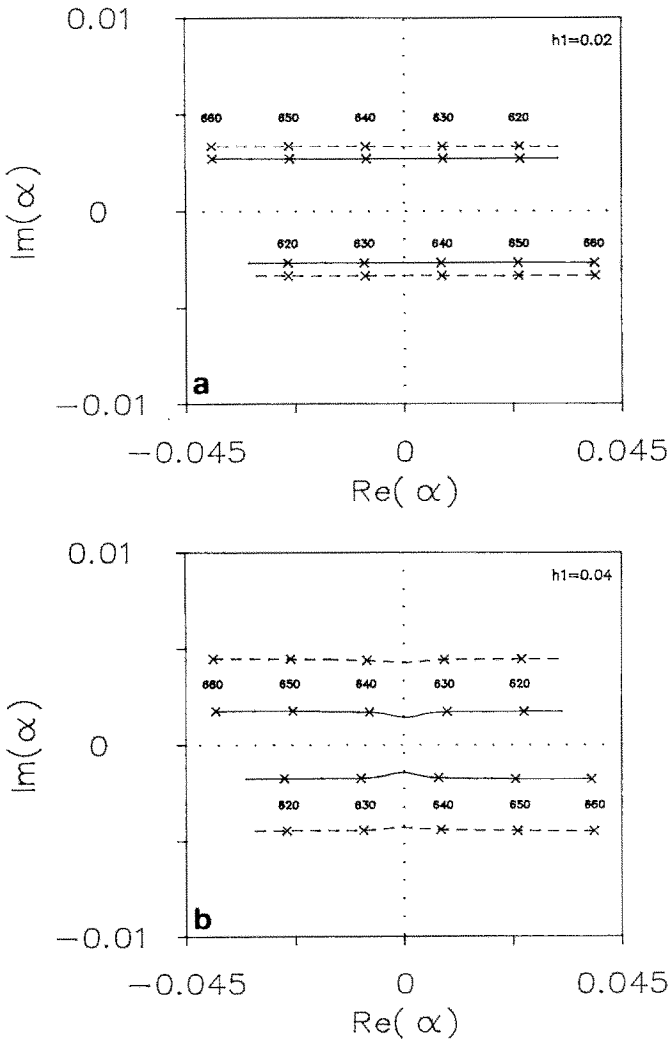


Fig. 1. (a–d) Trajectories of the poles (dashed lines) and zeros (solid lines) as a function of wavelength  $\lambda$  [nm] (shown with crosses) for different groovedepth values  $h_1$  [ $\mu\text{m}$ ]. Aluminum grating with sinusoidal profile and period  $0.63 \mu\text{m}$ . Dotted lines represent real and imaginary  $\alpha$ -axis.

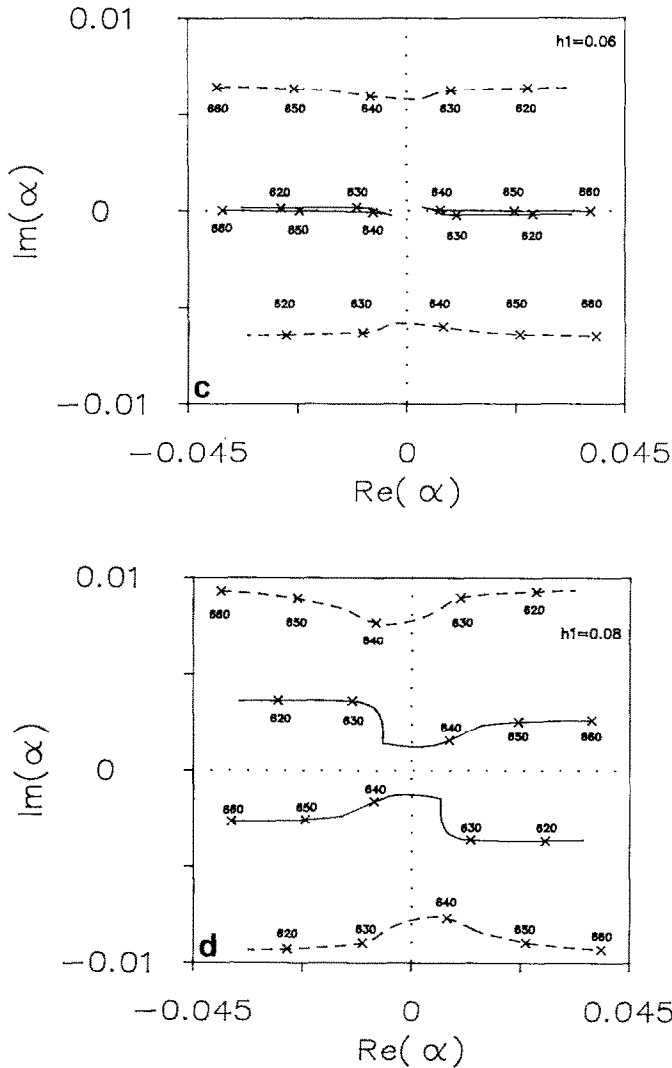


Fig. 1. Continued.

the trajectory of  $\alpha_0^z(\lambda)$  can cross the real  $\alpha$ -axis resulting in the zeroth value of reflectivity minimum (e.g. fig. 1c).

When  $\lambda$  is varied, the trajectory of the pole can approach  $\text{Re}(\alpha) = 0$ , and a simultaneous excitation of the oppositely propagating PSW's occurs. As the profile function  $f(x)$  contains only  $\pm 1$ st Fourier component, the direct coupling between the two plasmons is impossible. The grating is shallow ( $h_1/d < 0.13$ ) thus the indirect coupling (through the second-order processes)

is rather weak and does not affect the trajectory of the poles. Moreover, instead of splitting, attraction of the poles is observed: when the diffraction order in air is cut-off the losses decrease and  $\text{Im}(\alpha_0^{\text{p}})$  decreases, too.

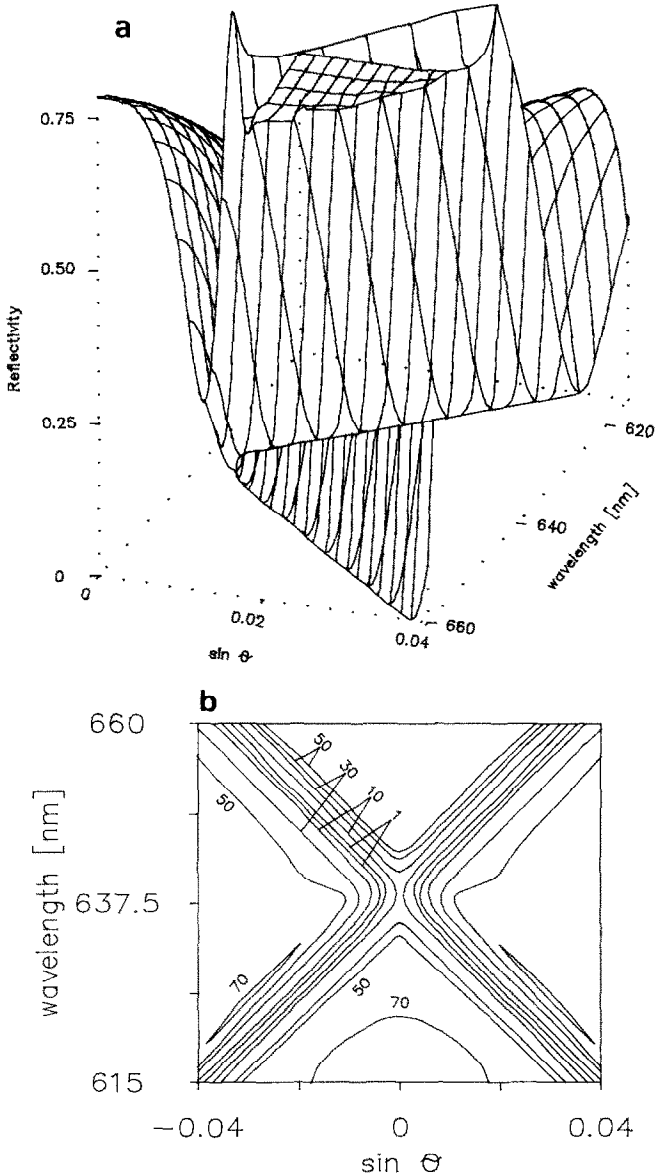


Fig. 2.  $\lambda$ - $\alpha$  dependence of the reflectivity for aluminum sinusoidal grating with period  $0.63 \mu\text{m}$  and groovedepth  $0.06 \mu\text{m}$ . (a) A 3D view with viewpoint situated at the lower side in order to visualize the trajectory of the reflectivity dip. (b) Contour plot of the reflectivity values (%).

The zeros have the same behavior, provided they are far enough from real  $\alpha$ -axis. Otherwise a strong interaction (repelling) of their trajectories is observed (fig. 1c with  $h_1 = 0.06 \mu\text{m}$ ). Such interaction of zeros, rather than poles, can be understood taking into account that all zeros of the zeroth reflected order are poles of the improper scattering matrix lying on one and the same improper Riemann sheet [8].

The evolution of general reflectivity surface in  $\lambda$ - $\alpha$  (or  $\omega$ - $k$ ) space corresponding to the pole-zero trajectories in fig. 1c is presented in fig. 2. Only the part of the surface for  $\alpha \geq 0$  is given, as it is symmetrical with respect to  $\alpha = 0$ . As there are no zeros around  $\alpha = 0$ , an  $\alpha$ -gap (i.e.  $k$ -gap) can be observed. On the other hand for the whole investigated spectral interval the zero is lying very close to the real axis and that is why there is no  $\omega$ -gap in the considered case. Here the trajectory of the reflectivity minimum in  $\omega$ - $k$  plane does not directly correspond to the trajectory of the pole, as condition (2) is no more satisfied.

### 3.2. Non-sinusoidal grating

The second example deals with a grating profile defined by

$$f(x) = (h_1/2) \sin(2\pi x/d) + (h_2/2) \sin(4\pi x/d). \quad (6)$$

The second term with amplitude  $h_2$  provides in a definite wavelength region a direct coupling between oppositely propagating PSW's. Spectral tracing of trajectories of poles and zeros in the complex  $\alpha$ -plane is presented in figs. 3a-3d for fixed  $h_2 = 0.02 \mu\text{m}$  and different values of  $h_1$ . Due to the strong direct coupling a strong repelling of pole trajectories is observed when  $\lambda/d \approx \text{Re}(\alpha^p)$ . As the amplitude of the second term in eq. (6) is one and the same and the coupling strength is determined predominantly by this term, the splitting of the trajectories ( $\max[\text{Im}(\alpha_0^p)]$ ) is almost independent of  $h_1$ . The trajectories of the poles "pull up" the zeros – in fact the strong direct coupling leads to the splitting of zeros, as well, because they are improper poles [8]. There are cuts in the trajectories of the zeros that take place at  $\lambda \approx 630.5 \text{ nm}$  – then the trajectories are crossing the cut in the complex  $\alpha$ -plane corresponding to the passing-off of radiation order in the upper medium [4,8].

In the coupling region the zeros are pulled away from the real  $\alpha$ -axis and an almost full annihilation of poles and zeros takes place. Thus there is a region in  $\lambda$  where no anomaly is observed, i.e.  $\omega$ -gap is formed in the  $\omega$ - $k$  dependence of reflectivity (fig. 4).

*Remark concerning the grating profile:* because the investigated gratings in which the well-pronounced dips in the reflectivity are observed are shallow, only the first-order processes are of noticeable effect. Thus different profiles with one and the same first- and second-order Fourier components are expected to generate almost identical reflectivity curves. Moreover, the grating

period and the wavelength interval are of one and the same order and higher harmonics are not expected to interact with incident light. From that point of view the profile function from eq. (6) with  $h_1 = 0.06 \mu\text{m}$  and  $h_2 = 0.02 \mu\text{m}$  is equivalent to the grating with an asymmetrical triangular profile with height  $h = 0.07788 \mu\text{m}$  and apex angle  $145.63^\circ$ . A comparison between the spectral dependences of normal incidence reflectivities for these two profiles is given in fig. 5; a very good coincidence is observed. In particular, a well-pronounced  $\omega$ -gap is formed.

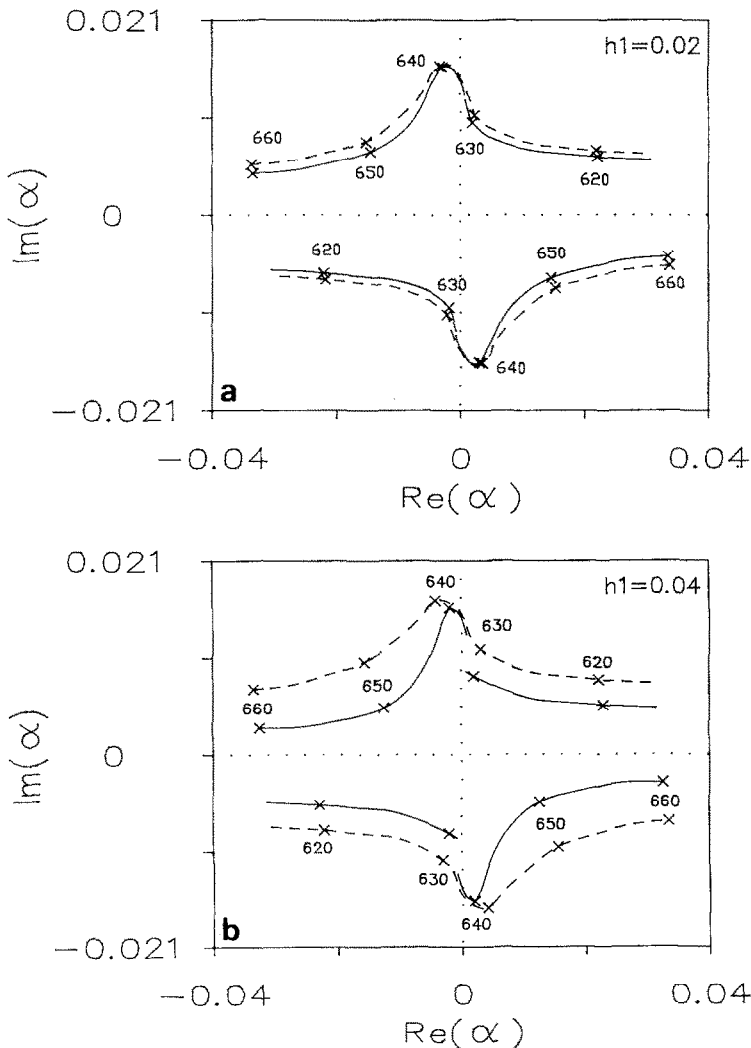


Fig. 3. Same as figs. 1a–1d but for grating with a profile given by eq. (6);  $h_2 = 0.02 \mu\text{m}$ .



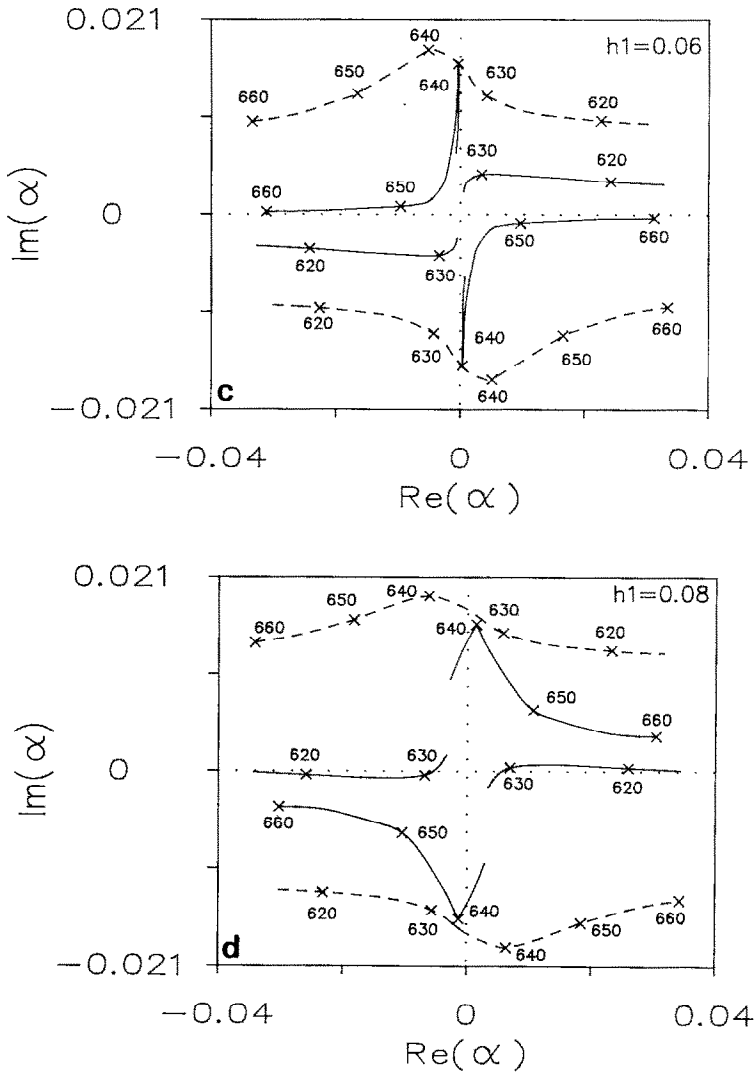


Fig. 3. Continued.

A natural question arises: which is of greatest importance for the formation of  $\omega$ -gap – the asymmetry of the grating profile or the strength of its second Fourier component. For this aim a symmetrical grating is considered having a  $\pi/2$  phase shift between the first and the second Fourier components:

$$f(x) = (h_1/2) \sin(2\pi x/d) + (h_2/2) \sin(4\pi x/d + \pi/2). \quad (7)$$

The resulting profile is shown in the insert of fig. 5b.

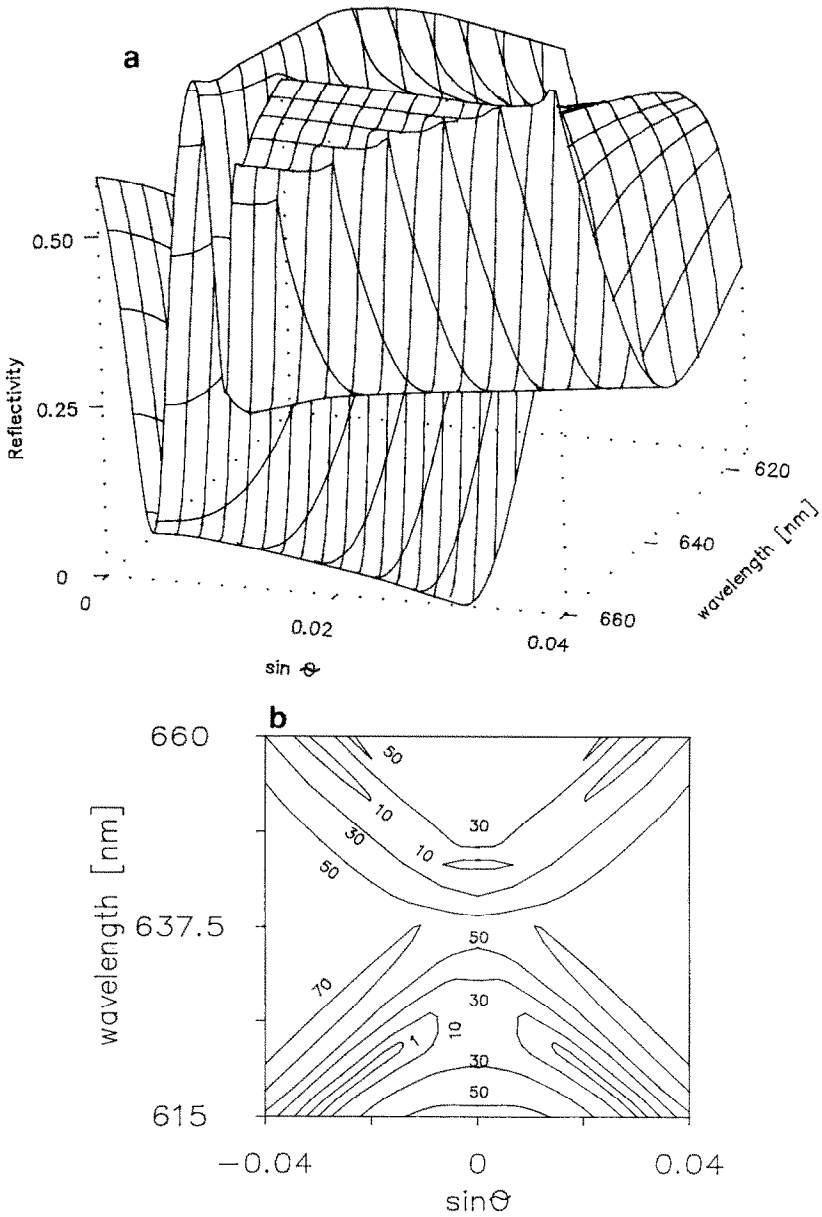


Fig. 4. Same as fig. 2 but for grating with a profile given by eq. (6);  $h_1 = 0.06 \mu\text{m}$ ,  $h_2 = 0.02 \mu\text{m}$ .

Again a well-pronounced  $\omega$ -gap can be observed. The main difference between the two sets of reflectivity curves presented in figs. 5a and 5b is the absence of a lower wavelength minimum at normal incidence for symmetrical

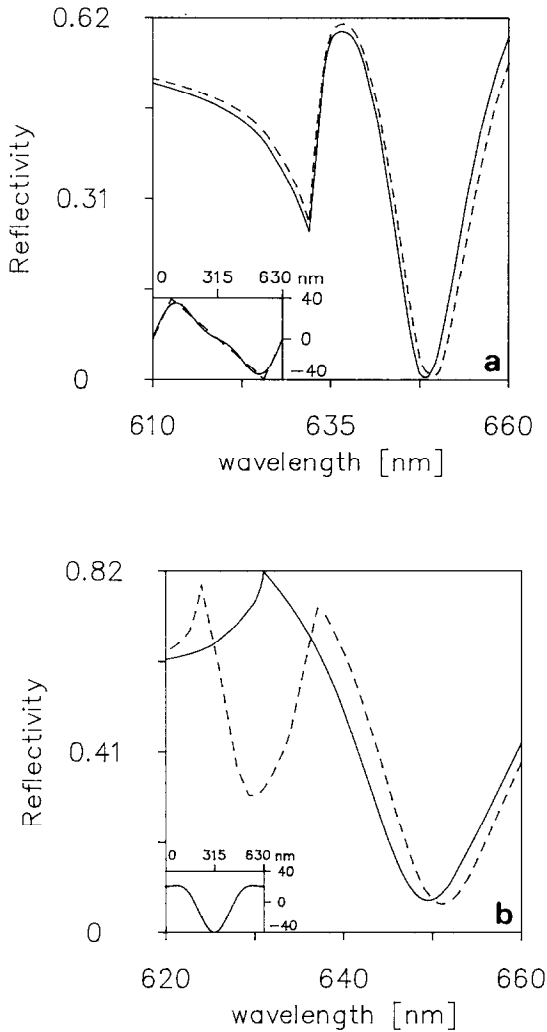


Fig. 5. Spectral dependence of the reflectivity, (a) Normal incidence for two gratings having mutually identical first two Fourier components: solid line – with profile given by eq. (6) with  $d = 0.63 \mu\text{m}$ ,  $h_1 = 0.06 \mu\text{m}$  and  $h_2 = 0.02 \mu\text{m}$ ; dashed line – with asymmetrical triangular profile with period  $0.63 \mu\text{m}$ , total groovedepth  $0.07788 \mu\text{m}$  and apex angle  $145.63^\circ$ . (b) Grating with profile represented by eq. (7) with  $d = 0.63 \mu\text{m}$ ,  $h_1 = 0.06 \mu\text{m}$  and  $h_2 = 0.02 \mu\text{m}$ : solid line – normal incidence; dashed line –  $\theta = 0.57^\circ$ . Different profiles are represented in the inserts of the figures.

grating. This phenomenon has already found its explanation in ref. [9] taking into account symmetry considerations. When the angle of incidence is not equal to zero (dashed curve in fig. 5b) the second dip can also be observed.

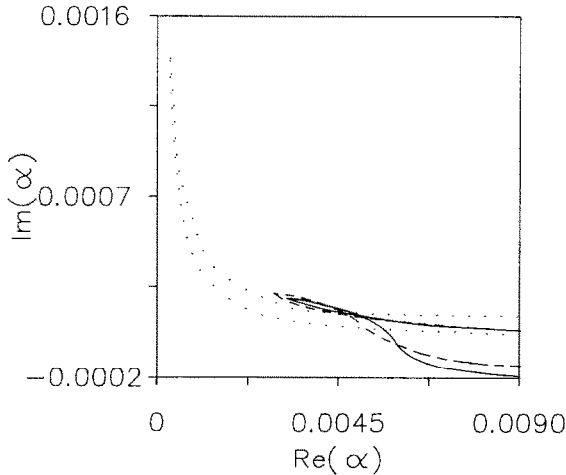


Fig. 6. Enlarged view of the trajectories of the zeros of reflectivity. Aluminum grating with period  $0.63 \mu\text{m}$  and profile given by eq. (6) with  $h_1 = 0.06 \mu\text{m}$ . Solid line:  $h_2 = 0$ , dashed line:  $h_2 = 0.002 \mu\text{m}$ , and dotted line:  $h_2 = 0.005 \mu\text{m}$ .

Thus the conclusion can be drawn that the formation of an  $\omega$ -gap is due to the strong direct coupling rather than to the asymmetry of the grating profile.

### 3.3. Transition between two types of gaps

Increase of  $h_2$  (responsible for the direct coupling) leads to a stronger and stronger splitting of poles. As a result a section of the trajectories of the zeros is pulled away from the real  $\alpha$ -axis (fig. 6). For small values of  $h_2$  (i.e. small direct coupling) the “vertical” (along the imaginary  $\alpha$ -axis) shift of  $\alpha_0^z$  is quite small (e.g.  $h_2 = 0$ ,  $h_2 = 0.002 \mu\text{m}$ ). In that case the  $\lambda$ - $\alpha$  dependence of the reflectivity resembles very much fig. 2. Thus in the case of a small direct coupling strength the  $k$ -gap exists. Increase of  $h_2$  pushes the trajectories of the zeros further into the complex  $\alpha$ -plane away from the real axis. Together with that the splitting along the real  $\alpha$ -axis is diminished. It means that for almost all values of angle of incidence lying close to the normal incidence there are values of wavelength responsible for almost real  $\alpha_0^z$ . Thus above some value of  $h_2$  the  $k$ -gap does not exist. On the other hand a spectral interval is formed for which the zeros are pushed away from the real axis, i.e. an  $\omega$ -gap is formed (e.g.  $h_2 = 0.005 \mu\text{m}$  in fig. 6 and  $h_2 = 0.02 \mu\text{m}$  in figs. 3c and 4).

## 4. Conclusion

On the basis of rigorous numerical tracing of spectral trajectories of poles and zeros in the reflectivity of metallic gratings it is shown that:

(1) an  $\omega$ -gap is formed when splitting of the poles (and zeros) takes place due to the existence of strong direct coupling of oppositely propagating plasmon surface waves,

(2) a  $k$ -gap is formed when there is no splitting of poles (very weak direct coupling), but a splitting and repelling of zeros lying near the real  $\alpha$ -axis exist.

## Acknowledgements

The author is thankful to Dr. Zs. Szentirmay (Central Research Institute for Physics, Hungarian Academy of Sciences) for bringing attention and inspiring interest for the subject. The author is also thankful to the referee who has made significant contributions to the paper with his important remarks. This paper is finished with the financial support of the Ministry of Culture, Science and Education under the contract No. 648.

## References

- [1] See for example: F. Toigo, A. Marvin, V. Celli and N.R. Hills, *Phys. Rev. B* 15 (1977) 5618; N.E. Glass, H.G. Weber and D.L. Mills, *Phys. Rev. B* 29 (1984) 6548.
- [2] D. Heitmann, N. Kroo, Ch. Schultz and Zs. Szentirmay, *Phys. Rev. B* 35 (1987) 2660; H. Jonsson, J.H. Weare, T.H. Ellis and G. Scoles, *Surface Sci.* 180 (1987) 353.
- [3] P. Tran, V. Celli and A.A. Maradudin, *Opt. Letters* 13 (1988) 530.
- [4] See for example: M. Neviere, in: *Electromagnetic theory of Gratings*, Ed. R. Petit (Springer, Berlin, 1980) ch. 5.  
D. Maystre, in: *Electromagnetic Surface Modes*, Ed. D. Boardman (Wiley, New York, 1982) ch. 17.
- [5] J. Chandezon, M.T. Dupuis, G. Cornet and D. Maystre, *J. Opt. Soc. Am.* 72 (1982) 839.
- [6] E. Popov and L. Mashev, *Opt. Acta* 33 (1986) 593;  
E. Popov and L. Mashev, *J. Mod. Opt.* 34 (1987) 155.
- [7] E. Popov, L. Tsonev and D. Maystre, *J. Mod. Opt.*, in press.
- [8] J.R. Andrewartha, J.R. Fox and I.J. Wilson, *Opt. Acta* 26 (1979) 197;  
L. Mashev and E. Popov, *J. Opt. Soc. Am.*, to be published.
- [9] M.G. Weber and D.L. Mills, *Phys. Rev. B* 31 (1985) 2510.